PHYSICAL REVIEW D

PARTICLES AND FIELDS

Measurements of the cosmic background radiation temperature at 3.3 and 9.1 mm

Giovanni De Amici, Chris Witebsky, George F. Smoot, and Scott D. Friedman

Space Sciences Laboratory and Lawrence Berkeley Laboratory, University of California,
Berkeley, California 94720

We report the results of measurements of the cosmic background radiation temperature at wavelengths of 9.1 and 3.3 mm. The 9.1-mm result, $T_{CBR} = 2.87 \pm 0.21$ K, is in good agreement with previous results and those obtained at longer wavelengths during the same experiment. The 3.3-mm result, $T_{CBR} = 2.4 \pm 1.0$ K, is consistent with previous measurements, but has a large uncertainty caused by uncertainty in the atmospheric emission.

According to the standard big-bang model, the spectrum of the cosmic background radiation (CBR) contains important information about the events and processes that took place in the early universe. The wealth of knowledge that a precise measurement of the spectrum would yield has been stressed in previous papers by several authors.[1−4] The short-wavelength spectrum has been measured recently,[5] but no attempt has been made to measure the CBR at long wavelengths in more than 12 years.

A systematic program, aimed at obtaining accurate measurements of the CBR temperature at five wavelengths (0.33, 0.91, 3, 6.3, and 12 cm), was carried out on 5 and 6 July, 1982. The observations were made at the Barcroft Laboratory (altitude 3800 m) of the White Mountain Research Station (California). This paper describes our measurements of the CBR temperature at wavelengths of 0.33 and 0.91 cm (90 and 33 GHz). An overview of the project, a description of the common apparatus, and a discussion of the results have been provided in a preceding paper.[6]

The accuracy of the previous measurements in the 0.3−1-cm wavelength range[6−8] has been limited by uncertainties in the atmospheric contribution and by systematic errors resulting from uncertainty in the instrument parameters. Improved microwave components have led to radiometers with greater sensitivity. Increased sensitivity allows us to make a complete measurement of the CBR and of atmospheric emission every few minutes, and thus reduces the uncertainty caused by changes in the atmosphere during a measurement sequence. Equally important, it increases our ability to measure and analyze the performance of the radiometers, and thereby helps us to evaluate and often reduce the systematic uncertainties in the measurement.

We determine the temperature of the CBR according to the formula

$$T_{A,CBR} = (T_{ZENITH} - T_{CL}) + T_{CL} - T_{ATM} \qquad (1)$$

by comparing the sky directly overhead with a liquid-helium-cooled load whose antenna temperature[7] is known to high accuracy. Each radiometer performs the comparison directly, using two antennas pointed in opposite directions. One antenna views the cold load below while the other observes the zenith above in order to measure the difference in their antenna temperatures. We add the antenna temperature of the cold load to the measured temperature difference to obtain the antenna temperature of the sky at the zenith T_{ZENITH}.

The important components of T_{ZENITH} are the CBR antenna temperature $T_{A,CBR}$ and the atmosphere's contribution to the zenith temperature T_{ATM}. T_{ATM}, which is large and variable due to water-vapor fluctuations, was determined by measuring the change in the sky's antenna temperature with zenith angle (and hence with atmospheric column density) and then fitting to an atmospheric model.[8] T_{ZENITH} also contains contributions from astronomical objects (Sun, Moon, and galactic sources), and from any emissive object in the sidelobes of the antenna. Low-sidelobe antennas and careful shielding reduce these last contributions to a negligible level. The Sun and Moon do not contribute significantly for measurements made at night with the Moon more than 15 degrees from the antenna beam axis. Galactic emission can be neglected at these wavelengths.

Figure 1 shows a schematic diagram of the 9.1-mm radiometer. The 3.3-mm system is smaller, but similar in all important characteristics. The corrugated-horn antennas [7.5° half-power beam width (HPBW)] used in the two radiometers are geometrically scaled versions of one another. The two oppositely directed antennas provide inputs to a Dicke superheterodyne radiometer, switched at 100 Hz. The instrument produces an output voltage pro-
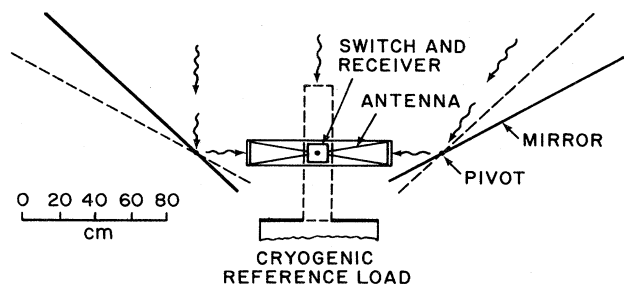
FIG. 1. Schematic diagram of the 9.1-mm radiometer. The instrument can be pointed horizontally for atmospheric measurements or vertically for measurements of T_{ZENITH}. The reflectors can be tilted to various angles to measure T_{ATM}.

portional to the two-second average of the difference in antenna temperature between the objects viewed by the two antennas. The antennas and the receiver are rigidly mounted and temperature controlled to provide mechanical and thermal stability. Operating characteristics are shown in Table I.

Each radiometer is mounted on bearings which allow the antennas to point either vertically or horizontally. The vertical orientation is used to measure the temperature difference between the sky and the cold load. The horizontal orientation, used for measurements of the atmosphere, directs the antenna beams at two reflectors made of foamed plastic panels faced with aluminum sheet. The reflectors pivot to redirect the beams upward at specified zenith angles.

The microwave absorber in the cold load has a physical temperature of 3.77 ± 0.01 K; the corresponding antenna temperatures are 2.01 ± 0.01 K at 3.3 mm and 3.03 ± 0.01 K at 9.1 mm. The cold load has cylindrical aluminum walls and two thin (18-micron) polyethylene windows over the top. The walls and windows add 0.10 ± 0.04 K at 3.3 mm and 0.06 ± 0.03 K at 9.1 mm, so the antenna temperature T_{CL} of the cold load is 2.11 ± 0.04 K at 3.3 mm and 3.09 ± 0.03 K at 9.1 mm.

Each radiometer also uses an ambient-temperature blackbody load for gain calibrations. These loads are made of ferrite-loaded plastic, cast into an array of cones

TABLE I. Operating parameters of the radiometers.

	3.3 mm	9.1 mm
Wavelength	3.3 mm	9.1 mm
Bandwidth	2 GHz	1 GHz
System noise	1600 K	800 K
Sensitivity	110 mK/Hz$^{1/2}$	80 mK/Hz$^{1/2}$
Gain stability	$\pm0.2\%$/night	$\pm0.6\%$/night
Radiometer offset	6.8 K	3.1 K
Antenna HPBW	7.5°	7.5°
Reflector size	122×91 cm	152×122 cm
Angles from	0, 40S, 50S	0, 30N/S
zenith for	(S refl.)	40 N/S
atmospheric	0, 40N, 50N	for each
scans	(N refl.)	reflector

and embedded in foam insulation. They have a reflection coefficient less than 2×10^{-3}.

The sequence of measurements used to determine $T_{A,\text{CBR}}$ lasted 4 minutes with the 3.3-mm radiometer and 5 minutes with the 9.1-mm radiometer. The sequences were repeated for runs of 40 to 60 minutes, twice per night. Each sequence evaluated three quantities: (1) the temperature difference between the zenith and the cold load, (2) the temperature difference between the ambient-temperature load and the cold load (to calibrate the radiometer gain), and (3) the temperature difference between the zenith and the sky at one or more zenith angles (to measure the atmospheric contribution). The radiometer output, calibrator temperatures, and system housekeeping data were recorded on magnetic cassette tape and by hand.

Each sequence is analyzed individually, using Eq. (1). Radiometer output voltages are averaged over each measurement and constant offsets are removed. The radiometer gain is calculated from measurements of the cold and ambient loads. A $7\pm1\%$ correction is made for gain saturation in the 9.1-mm radiometer; no correction is needed for the 3.3-mm radiometer. The temperature difference $(T_{\text{ZENITH}}-T_{\text{CL}})$ is determined from the sky/cold-load measurements and the measured gain.

The atmospheric model used to compute T_{ATM} from measurements at different zenith angles is approximately a secant law, but also includes the effects of atmospheric curvature and self-absorption, and antenna beam width (the difference between the model and a pure secant law is 90 mK at 9.1 mm and 330 mK at 3.3 mm). We also correct for the variation in the emissivity of the aluminum reflectors with the angle of incidence (up to 130 mK).

Typical results of our atmospheric measurements are

$$T_{\text{ATM}}=5.00\pm0.14 \text{ K} \quad \text{at } 9.1 \text{ mm },$$

$$T_{\text{ATM}}=12.3\pm0.8 \text{ K} \quad \text{at } 3.3 \text{ mm },$$

where the values are the averages of the results obtained during one night of observation and the quoted errors are the uncertainties in the values from an individual measurement sequence. The average temperature value at 9.1 mm is larger than our theoretical estimate based on measurements at other wavelengths,[8] but still in marginal agreement with it. It falls between the values previously obtained at the same location in the 9-mm range (4.62 K, Ewing et al;[9] 6.6 K, Wilkinson[10]). Our 3.3-mm atmospheric measurement is in good agreement with previous values.[11–12]

Statistical errors are caused by radiometer noise and by fluctuations in the radiometric temperature of the atmosphere. The rms variation in $T_{A,\text{CBR}}$ is approximately 130 mK at 9.1 mm and 250 mK at 3.3 mm. Radiometer noise causes a 40 to 50-mK uncertainty; the rest is due to atmospheric fluctuations (Fig. 2).

Systematic errors come from uncertainties in the correction terms (Table II). The most important one results from uncertainties in the zenith angles used in atmospheric measurements, due to antenna misalignment or inaccurate reflector positions. For instance, a 10-arcminute error in the zenith angle causes T_{ATM} to be in error by 50 mK at 9.1 mm and 120 mK at 3.3 mm. Sun-
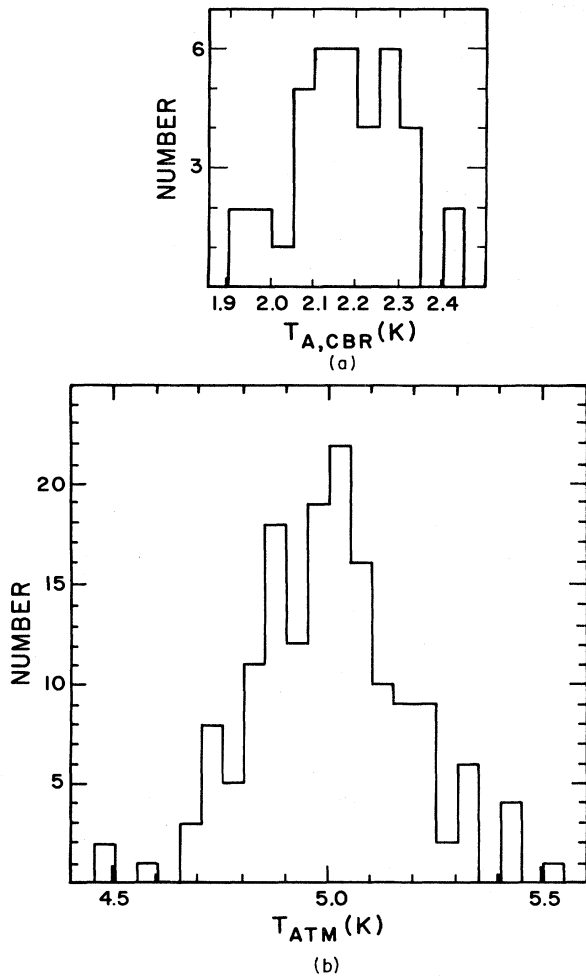
FIG. 2. Histograms of the results at 9.1 mm obtained during the night of 5 July, 1982. (a) Antenna temperature of the CBR, $T_{A,\text{CBR}}$—the mean value is 2.18 K and the rms variation of the 38 data points is 0.13 K. (b) Atmospheric antenna temperature T_{ATM}—the mean value is 5.00 K and the rms variation for 157 observation is 0.37 K.

TABLE II. Systematic errors and correction terms (kelvins).

Radiometer wavelength	3.3 mm	9.1 mm
Cold-load temperature:		
LHe antenna temperature	2.01±0.01	3.03±0.01
Wall emission	0.03±0.03	0.04±0.03
Window emission	0.07±0.03	0.016±0.003
Reflection from load	<u>0.001</u>	<u>0.009</u>
Total	2.11±0.04	3.09±0.03
Vertical atmosphere:		
Typical values	12.3±0.8	5.00±0.14
Uncertainties from		
zenith-scan pointing	0.6	0.12
horizontal antenna		
sidelobes	0.01	0.01
emission from Moon		
and galaxy	0.001	0.003
diffraction over		
reflector's edge	0.008	0.008
rms of an individual		
sequence	0.2	0.14
Vertical flip offset	0.3	0.10
Horizontal flip offset	0.03	0.015
Magnetic field offset		
(per Gauss)	0.0015	0.001
Sidelobes from		
vertical antenna	0.001	0.001
Gain saturation (%)	0±2	7±1

light shining on the 3.3-mm radiometer warped its reflectors by approximately 1.5°, causing a large uncertainty in T_{ATM}. The 9.1-mm radiometer experienced a similar problem, causing an anomalously large spread (500 mK) in the atmospheric temperatures measured at different zenith angles on 6 July. Therefore, the 9.1-mm data from that night are not included in this analysis.

Both radiometers showed offsets due to asymmetries in the horns and/or the ferrite switch ports. These offsets have been subtracted from the data during the analysis, under the assumption that they are independent of the radiometer orientation. A systematic error results if the offset changes with the radiometer orientation ("flip" offset). Flip offsets may result from changes in the orientation of the ferrite switch with respect to the earth's magnetic field, or they may be caused by mechanically induced stresses on the waveguide components. Tests conducted in Berkeley indicate that the magnetically induced

offset is less than 2 mK/G for both radiometers.

Measurements of the flip offset have been made with the antennas pointed horizontally; when the radiometer is rotated 180°, the change in the output is less than 30 mK. This result suggests that the effect should be small in all radiometer orientations, and that the sky measurements obtained with the two antennas can be combined.

We have not made accurate direct measurements of the flip offset with the antennas pointed vertically, because we do not have a well-calibrated cold target to put in front of the upward-looking antenna. However, we do compare the offsets in the vertical and horizontal orientations to check their consistency. To do so, we compute the average of the offset in the two-vertical orientation, and subtract it from the offset obtained when the antennas are pointed horizontally. The differences between the vertical and horizontal offsets is less than 100 mK for the 9.1-mm instrument and 300 mK for the 3.3-mm one.

These uncertainties are included in the analysis as a part of the systematic error. Systematic errors also result from drifts in the switch offset and radiometer gain during a measurement sequence, from errors in the various correction terms, and from emission from objects in the sidelobes of the antenna. None of these smaller uncertainties is estimated to be greater than 40 mK (Table II).

The average of $T_{A,\text{CBR}}$ resulting from all the measuring sequences is converted to a thermodynamic temperature T_{CBR} to give the final result

$$T_{\text{CBR}} = 2.87 \pm 0.21 \text{ K} \quad \text{at 9.1 mm} ,$$

$$T_{\text{CBR}} = 2.4 \pm 1.0 \text{ K} \quad \text{at 3.3 mm} ,$$

where the quoted errors are the statistical and systematic errors summed in quadrature. At 9.1 mm, statistical uncertainty contributes approximately 70 mK to the total error; the remainder is due to systematics. At 3.3 mm the error is almost entirely due to pointing uncertainty.

Our value of T_{CBR} at 9.1 mm is in good agreement with the published results in this wavelength range.[9,10,13] It is also intermediate between the temperature measured by Woody and Richards[5] at shorter wavelengths and the average of all the previous ground-based measurements,[6] and falls within one standard deviation of both. At 3.3 mm, our results are consistent with previous measurements,[11–12] but pointing uncertainties prevent us from concluding anything more definite.

[1]R. Weiss, Annu. Rev. Astron. Astrophys. 18, 489 (1980).
[2]L. Danese and G. De Zotti, Riv. Nuovo Cimento 7, 277 (1977).
[3]R. J. Bontz, R. H. Price, and M. P. Haugan, Astrophys. J. 246, 592 (1981).
[4]L. Danese and G. De Zotti, Astron. Astrophys. 68, 157 (1978).
[5]D. Woody and P. Richards, Phys. Rev. Lett. 42, 925 (1979).
[6]G. Smoot, G. De Amici, S. Friedman, C. Witebsky, N. Mandolesi, R. B. Partridge, G. Sironi, L. Danese, and G. De Zotti, Phys. Rev. Lett. 51, 1099 (1983).
[7]Antenna temperature is defined by the equation $P = kT_A B$, where P is the incoming power, T_A is antenna temperature, B is radiometer bandwidth, and k is Boltzmann's constant. In the Rayleigh-Jeans limit, the antenna temperature of a blackbody is equal to its thermodynamic temperature.
[8]R. B. Partridge, et al., this issue, Phys. Rev. D 29, 2683 (1984).
[9]M. S. Ewing, B. F. Burke, and D. H. Staelin, Phys. Rev. Lett. 19, 1251 (1967).
[10]D. T. Wilkinson, Phys. Rev. Lett. 19, 1195 (1967).
[11]P. E. Boynton, R. A. Stokes, and D. T. Wilkinson, Phys. Rev. Lett. 21, 462 (1968).
[12]M. F. Millea et al., Phys. Rev. Lett. 26, 919 (1971).
[13]V. I. Puzanov, A. E. Salomonovich, and K. S. Stankevich, Astron. Zh. 44, 1129 (1967) [Sov. Astron. 11, 905 (1968)].